

## Heat transfer in plagioclase feldspars

Joy M. Branlund<sup>1</sup> and Anne M. Hofmeister<sup>2</sup>

<sup>1</sup>Southwestern Illinois College, Granite City, Illinois 62040 U. S. A.

<sup>2</sup>Washington University in St. Louis, St. Louis, Missouri 63130 U. S. A.

Email: Joy.Branlund@swic.edu

### Abstract

Laser Flash Analyses (LFA) of oriented sections of six natural plagioclase crystals provide thermal diffusivity ( $D$ ) as function of temperature (to ~1300-1500 K) and composition ( $An_{5-95}$ ). Plagioclase has low thermal diffusivity; our measurements indicate that plagioclase is more insulating than other major igneous rock-forming minerals. Over much of the solid solution, room temperature  $D$  is 0.979 to 0.751 mm<sup>2</sup>/s along **c**, 0.919 to 0.722 mm<sup>2</sup>/s along **b**, and 0.632 to 0.868 mm<sup>2</sup>/s perpendicular to **b** and **c**. The directionally averaged  $D$  is 30-45% lower than  $D$  of Amelia albite. Thermal conductivities calculated using measured  $D$  values are almost the same for all samples with  $18 \geq An \leq 65$ , being about 1.5 - 1.9 Wm<sup>-1</sup>K<sup>-1</sup> and changing little with temperature. Increasing Al-Si disorder causes  $D$  to decrease with increased An content, although sample structure causes more ordered samples to have higher  $D$  than more disordered samples. Structure dictates whether  $D$  along the **b** axis is greater or less than that along **c**, possibly because ordering in An-like domains increases  $D$  along **c** relative to **b**. Inflections in  $D(T)$  are connected with lattice distortion during heating, and occur near temperatures expected for phase transitions; for example, the lattice stretch occurring at the temperature of the transition to  $C\bar{1}$  structure lowers  $D$ . Likewise, lattice distortion during heating decreases  $D$  in albite along **c** but has little impact on  $D$  in the other directions. The anharmonic lattice effects that dictate both thermal

expansivity and  $D$  are swamped by effects of disorder; the latter plays a major role in heat transport in plagioclase.

**Keywords:** plagioclase, heat transfer, thermal diffusivity, thermal conductivity, laser-flash analysis, high-temperature studies

## Introduction

Solving many geologic problems requires understanding the thermal nature of Earth's crust and mantle, and thus knowledge of relevant mineral heat transfer properties (thermal conductivity ( $k$ ) and thermal diffusivity ( $D$ )). Therefore, we have been building a database of mineral thermal diffusivities measured with Laser Flash Analysis (LFA). To date, several glass and mineral systems have been probed, including quartz, perovskite, olivine, clinopyroxene, orthopyroxene, garnet and spinel (Branlund and Hofmeister 2007; Hofmeister 2010; Pertermann and Hofmeister 2006, 2008; Hofmeister 2011, 2006, 2007). Data on low albite and low sanidine have been published (Pertermann et al. 2008; Hofmeister et al. 2009), but more-calcic plagioclase data are lacking. Given that feldspar is the most common rock-forming mineral, and plagioclase is prevalent in intermediate and mafic igneous rocks, it is especially important to characterize heat transfer in plagioclase.

Plagioclase minerals are structurally complex (Figure 1). At high temperature, a true solid solution exists between the sodic and calcic end members of the plagioclase series, albite ( $\text{NaAlSi}_3\text{O}_8$ ) and anorthite ( $\text{CaAl}_2\text{Si}_2\text{O}_8$ ). Low albite is ordered such that Al always resides on the  $\text{T}_1\text{O}$  site, forming a  $C\bar{1}$  structure. With increased temperature, Al can diffuse to other sites and albite disorders, forming high albite (still  $C\bar{1}$ ). At a higher temperature, the framework shears leading to a partially ordered monoclinic structure ( $C2/m$  space group) (Parsons 2010). In pure anorthite, each Al is surrounded by four Si and vice versa; the alternating layers of Si and Al

tetrahedra double the length of the **c**-axis in the crystallographic unit cell (McConnell 2008);

Like low albite, anorthite exhibits long-range order. Unlike albite, anorthite remains perfectly ordered (with the  $I\bar{1}$  structure) until melting. At low temperature (below about 500 K), the anorthite lattice distorts around Ca atoms, creating a  $P\bar{1}$  structure. Charge imbalances caused by Na-Ca substitution in anorthite-albite are counteracted by Al-Si exchange. Atomic ordering becomes complicated because Al-O-Al bonds are energetically expensive; intermediate plagioclase therefore consists of planar subdomains with slightly different structures, and these antiphase domains combine to form incommensurate superstructures. The two main intermediate structures are the more Ab-rich  $e_2$  and the more An-rich  $e_1$  plagioclase, so named because of  $e$  reflections that appear in single-crystal x-ray photographs. McConnell (2008) proposed that  $e_2$  plagioclase contains alternating domains of albite-like ( $C\bar{1}$ ) and anorthite-like ( $I\bar{1}$ ) structures, whereas the  $e_1$  phase contains alternating incommensurate layers of ordered and partially ordered  $I\bar{1}$  structures. The widths of the domains are on the order of 20-50 nm, and orientations vary with An-content and temperature (e.g., Carpenter 1991; Grove 1977). At low temperatures, miscibility gaps exist in the solid solution, and intergrowths of the different structures form, creating peristerite ( $C\bar{1}$  and  $e_2$ ), Bøggliid ( $e_1 + e_2$ ) and Hüttenlocher ( $e_1 + I\bar{1}$ ) intergrowths (Figure 1). It is likely that the entire solid solution, with the exception of the two end members, is immiscible at temperatures  $< \sim 400$  K (Parsons 2010). Because atomic diffusion is very sluggish in plagioclase, many samples retain a metastable structure (either  $C\bar{1}$ ,  $I\bar{1}$ ,  $e_1$  or  $e_2$ ) upon cooling. Only very slowly cooled plutonic samples and metamorphic samples will possess the intergrowths, whereas volcanic plagioclase are more disordered with structures that may reflect high temperature solid solution. Plagioclase therefore does not simply fall into a

“high” versus “low” category, but exhibits a wide range of order-disorder reflecting varied cooling histories.

More uncertainty exists in the low temperature portion of Figure 1 than in the upper due to sluggish kinetics. Locations of the upper phase boundaries are affected by Or contents. For example, adding K lowers  $T$  of the low to high  $C\bar{1}$  transition as well as the solidus (Parsons 2010). Water also alters the solidus, which decreases with increased  $P_{H_2O}$  by up to 400 K (Johannes et al. 1994).

In this study, we measure thermal diffusivity of natural plagioclase with compositions ranging from  $An_5$  to  $An_{95}$  at different temperatures, thus quantifying heat transfer for several different plagioclase chemistries and structures.

## Methods

### Samples

Low albite from Amelia County, Virginia, was previously studied along with Ab and An glasses (Hofmeister et al. 2009; note, the low albite was mistakenly called high albite in that paper). To this we add data from eight natural plagioclase samples with higher An contents, six of which were analyzed to high temperature (Table 1).

Except for FMA and FLC, each crystal was cut along three orthogonal directions. Two sections were cut parallel to (001) and (010). A third section cut perpendicular to these two faces is designated “ $\perp$ ” because plagioclase is triclinic; the perpendicular face is not (100). Values presented for (001) therefore quantify heat flow along **c** while (010) quantifies heat flow along **b**. Although **a** is almost perpendicular to **b**, it is oblique to **c** (angles range from 115.5°-116.3°), thus the perpendicular orientation does not quantify heat flow along **a**. The two orientations of

FMA were cut from two different crystals. Due to cracking during sample preparation, the third orientation ( $\perp$ ) was not prepared. Due to small sample size, only two orientations of FLC could be prepared.

Sections were ground into discs about 1 cm in diameter and less than 1 mm thick. The top and bottom of each disc were polished to be parallel. Optical microscopy was used to identify any inclusions and twinning. Before analyzing  $D$ , samples were sputter coated with platinum and then spray coated with graphite. The graphite coating maximizes energy absorption, and ensures that absorbed energy is spread across the surface. The platinum coating helps reduce the amount of direct (or ballistic) radiation through these transparent samples.

Chips from each sample were analyzed using wavelength-dispersive spectroscopy (WDS) on the JXA-8100 electron microprobe at Washington University in St. Louis to quantify major element chemistry. Accelerating voltage was 15 kV, beam current was nominally 25 nA, beam diameter was 1  $\mu\text{m}$ , and counting times were near 30 s. Various oxide standards were used for calibration. Measurements of three points were averaged to give the chemical formulas of plagioclase samples (Table 1).

### **Measurement of thermal diffusivity**

Thermal diffusivity was measured with the Netzsch LFA427, ~~a laser flash apparatus~~. The instrument heats the sample's base briefly with a laser pulse, and records changes in emissions from the top of the sample using a remote IR detector. Basically,  $D$  is calculated using the time taken for the heat from the pulse to travel through a sample of given thickness. This technique is preferred because no contacts exist between thermocouples and the sample; such contacts limit measurements to  $\sim 1200$  K and provide an additional thermal resistance that artificially lowers measured  $D$  values. LFA accounts for the shape of the laser pulse and removes

unwanted ballistic radiative transfer using the mathematical model of Mehling et al. (1998). For details, see Branlund and Hofmeister (2007).

Thermal diffusivities of plagioclase samples were measured at 100 K increments from room temperature up to between 1150-1550 K. FMA was measured at smaller increments in an attempt to capture the  $P\bar{I}$  to  $I\bar{I}$  transition. At each temperature step, at least three measurements were collected and averaged. Measurements with poor fits between the model and signal were not included in the average. Graphs presented herein show the average of successful measurements. Due to its small size,  $D$  of sample FSU $\perp$  could only be measured at room temperature. Samples FLT and FLC were also measured only at room temperature.

## Results

Plagioclase  $D$  generally decreases with temperature (Figure 2) and can be fit with a polynomial, namely:

$$D = \frac{1}{A + BT + CT^2 + ET^3} \quad (1)$$

Coefficients  $A$ ,  $B$ ,  $C$  and  $E$  for the different samples are given in Table 2.

Thermal diffusivity decreases with increased An content (Figure 3). For intermediate values of An, the  $D$  values are very similar; from An<sub>10</sub> and An<sub>95</sub>, room temperature  $D$  decreases from 0.979 to 0.751 mm<sup>2</sup>/s along **c** and 0.919 to 0.722 mm<sup>2</sup>/s along **b**. For comparison,  $D$  along **b** in pure albite is 1.689 mm<sup>2</sup>/s (Hofmeister et al. 2009). Albite's measured value of  $D$  along **c** of 1.354 mm<sup>2</sup>/s is likely too low; because that section was cut too thick, heat was probably lost through the sample's edges. Fracturing along cleavages prohibited preparation of a thinner sample.

For albite, even considering possible errors due to sample thickness,  $D$  along **b** (measured using (010) sample) is higher than along **c** for all temperatures measured (Figure 2a; Hofmeister et al. 2009). This is not the case for all other plagioclase samples studied. Like albite,  $D$  in sample FSU is significantly higher along **b** than **c** (Figure 2b). Although samples FLL and FBM also have greater  $D$  along **b** than **c**,  $D$  values are difficult to distinguish given experimental uncertainty, at least within certain temperature ranges. For sample FBM,  $D_{010}$  and  $D_{001}$  are similar from room temperature up to 768 K, such that  $D$  values diverge as temperature increases (Figure 2a). The  $D$  values along **b** and **c** for FMA are also similar for the measured temperatures (Figure 2b). Samples FON and FLN both had  $D_{001} > D_{010}$  at lower temperatures, although the  $D$  values crossed over, so that  $D_{010} > D_{001}$  at higher temperatures.

Except for FON and FLN, samples did not change appearance when compared before and after heating in the LFA. During LFA, sample FON was heated above its melting temperature. At about 1580 K, large peaks of direct radiation were detected in FON001 and FON $\perp$ , suggesting that these samples cracked, probably during the growth of lower density melt pockets. Although intact, both samples were netted with two sets of microscopic fractures that formed at angles between 40° to 60° from the **a-c** plane. FON001 had a higher density of cracks, as well as two larger cracks, one ending in a conchoidal fracture, near the sample's edge. There was no evidence wholesale flow (no change in sample shape, for example). However, inclusions visible in this sample pre-heating were not visible after LFA runs, and chains of dark, small dots (glass) appeared mostly along (001) cleavages in FON $\perp$  and along fractures in FON001.


Thermal diffusivity decreases or is constant with temperature at all temperatures measured with four exceptions. Thermal diffusivity increases significantly above 1300 K in FLN001 and FLN010 ( $D$  increases 7-11% from 1320 to 1420 K) (Figures 2b and 4).

Furthermore, additional measurements made on cooling show that in both FLN001 and FLN010,  $D$  remained higher upon cooling, at least until a temperature of  $\sim 800$  K. Sample FLN $\perp$  was not analyzed to as high a temperature as the other two orientations; it might very likely show a similar increase in  $D$  if analyzed at higher temperatures. The recovered sample contains two sets of fractures, one that lines up with ilmenite inclusions. FLN $\perp$  also cracked during analysis. The samples likely cracked on cooling, explaining the lower  $D$  measured during cooling below  $\sim 800$  K. The cracks also lead to lower room temperature  $D$  measured at a later date (diamond and plus sign in Figure 4).

Sample FON001 has a 5% increase in  $D$  from 1260 to 1460 K (filled gray circles in Figure 2a). That  $D_{001}$  increases following premelting from 1260 to 1460 K may result from dehydration. FMA001 also increased by about 5% from 830-1050 K.

### **Room-temperature thermal diffusivity and plagioclase structure**

Thermal diffusivity measurements may provide additional insights on plagioclase structure, the complexity of which is compounded by the sluggish kinetics (several samples retain their high temperature structures) and possible effects of variable amounts of K substituting for Na, or for Fe in either cation site, as well as small amounts of water or hydroxyl.

Thermal diffusivity of albite is much higher than  $D$  of other members of the plagioclase series. Likewise, albite is the only sample analyzed that should be well ordered at room temperature. The addition of Al in more Ca-rich samples reduces order, and hence reduces  $D$ . Likewise, in intermediate plagioclase, more ordered samples (FON, FLN, FLC) have higher room temperature  $D$  than the more disordered samples (FLL and FBM) (Figure 3). 



The direction of maximum  $D$  seems to depend on plagioclase structure, and crossovers in  $D^{-1}(T)$  plots occur at similar temperatures as plagioclase phase changes (Figure 5). For samples with  $C\bar{1}$  symmetry,  $D_{010} > D_{001}$ . For all other structures,  $D_{001} > D_{010}$ . In phases with a  $C\bar{1} + e_2$ , the direction of maximum  $D$  depends on the relative amounts of the two phases, which depends on An content. Samples with low An content such as FSU ( $An_5$ ) will have  $D_{010} > D_{001}$ , whereas samples with higher An content such as FON ( $An_{19}$ ) will have  $D_{001} > D_{010}$ . The division between these high and low An contents corresponds to the position of the  $C\bar{1} \leftrightarrow e_2$  boundary extrapolated to lower temperatures. The An-dependent switch in orientation of maximum  $D$  may suggest that development of the anorthite-like component of the superstructure increases  $D$  preferentially along  $c$ . This would occur if antiphase domains orient such that  $c$  resides almost entirely in the more-ordered domain.

### Thermal diffusivity and temperature-dependent structural changes

Several of the inflections in the  $D^{-1}(T)$  plots occur at the same temperatures <sup>of phase</sup> ~~of~~ <sup>observed in XRD.</sup> changes. Because LFA heating times are too fast to allow for Al-Si diffusion, the LFA results suggest that heating causes lattice strain that precedes atomic diffusion; it is not atomic diffusion that solely strains the lattice. However, slow Al-Si diffusion prevents lattice relaxation upon cooling. Fast heating can therefore result in structural changes that are not preserved upon cooling. If such structural changes exist, we expect to observe them in other fast-heating experiments. Benisek et al. (2009) noticed no inflections in their measurements of heat capacity. However, these authors used high structural state plagioclase and made measurements to only 800 K, too low to see the inflections we observed for our disordered samples. Foit and Peacor (1973) noticed instantaneous and reversible changes in lattice constants of Miyake anorthite

measured with x-ray diffractometry, and suggested the domain texture changed during heating without Al-Si diffusion. Likewise, Tribaudino et al. (2010) observed the  $P\bar{1}$  to  $I\bar{1}$  transition in unit-cell volume measurements of  $An_{100}$  using powder diffraction. Inflections are not apparent in volume data of samples with lower An contents (Tribaudino et al. 2010 and Hovis et al. 2010). However, this not rule out the existence of inflections in measurements of lattice constants that average out in volume calculations.

The fits to albite  $D^{-1}(T)$  ~~work~~ well to describe the data except for the measurement of (010) at 1300 K (Figure 6a). This temperature corresponds to the transition from  $C\bar{1}$  to  $C2/m$  (Figure 1). Similarly, data for FSU can be fit at temperatures below  $\sim 1250$  K (Figure 6b), the temperature expected for the  $C\bar{1} \leftrightarrow C2/m$  transition (1290 K; McConnell 2008). The inflections occurs at about 1100 K in the  $D^{-1}(T)$  plot for (001), which is lower than that for (010), suggesting that strain of the **c**-axis precedes deformation of the **b**-axis. This may also explain why the phase transition was observed to be gradual, the sample becoming more like  $C2/m$  with heating (Prewitt et al. 1976).

Each component of the peristerite intergrowths in FON should deform independently. If the more Ab-rich component (with a low  $C\bar{1}$  structure) restructures at a different temperature than the intermediate  $e_2$  structure, multiple inflections could exist in the data. The inflection seems to occur over a range of T from 650-800 K corresponding to the expected change from the intergrowths to  $C\bar{1}$  (Figure 6c).

The crossover of  $D_{010}$  and  $D_{001}$  also results from the change in structure to  $C\bar{1}$  symmetry, even though the crossover temperature for sample FON is hard to pinpoint. The measured  $D$  values for FON001 are slightly larger to 868 K, and by 976 K diffusivity is larger along (010) than along (001), but error bars for  $D$  along the two orientations overlap between 378 and 996 K.

Thermal diffusivity of FON001 and FON $\perp$  drop drastically between 1200 and 1300 K., while  $D_{010}$  decreases slightly at the same temperature. The melting temperature for this composition is about 1400 K (McConnell 2008). Although the presence of OH and K will lower the solidus (Johannes et al. 1994; Parsons 2010), the decrease in  $D$  is consistent with the glass transition as seen by the LFA occurring at temperatures about 100 K lower than the melting temperature (Hofmeister et al. 2009). Because the melting temperature of plagioclase increases with An-content (Figure 1), the more Ab-rich component of the peristerite intergrowth will melt first. Because peristerite intergrowths parallel  $\sim(010)$ , melt will form in the **a-c** plane, and therefore affect  $D_{\perp}$  and  $D_{001}$  more than  $D_{010}$ . As further evidence for differential melting of peristerite, melt (as beads of glass seen in recovered samples) aligns with the (001) cleavage in FON $\perp$ . Beads of glass do not align with (100) in FON001, but follow fractures. This might be expected if melt formed along **a** but then accumulated in fractures. At 1460 K, enough melt exists to crack the sample, allowing direct radiation through the sample that aborted the run. The melting of only one component of the intergrowth reminds us that the structural changes seen by LFA are not accompanied by any chemical diffusion.

The crossover temperature of FLN is about 850 K, which matches the predicted transition from the Bøggliid intergrowth ( $e_1+e_2$ ) to a high  $C\bar{1}$  structure (about 886 K) (Figure 6d). The  $e_1$  portion of the structure should alter to  $C\bar{1}$  at a lower temperature than the  $e_2$  phase, which explains the width of the transition in temperature space. Above this temperature (in the  $C\bar{1}$  stability field),  $D$  of FLN is considerably lower than for other samples (Figure 2b), until about  $\sim 1400$  K, where  $D$  of both orientations increase to values similar to the other plagioclase samples of about  $0.6 \text{ mm}^2/\text{s}$ . Some aspect of FLN's structure, perhaps the Bøggliid intergrowths, restricts  $D$ . As temperature increases, the structure flexes, and by 1600 K returns to that expected for  $C\bar{1}$

plagioclase with intermediate An values. The thermal history of the sample might also be responsible for the reset of  $D$  at high temperature. Although originally plutonic, the slowly cooled anorthosite intrusions were later metamorphosed. Strain imparted during metamorphism might have overprint the lattice in a manner that affects  $D$ .

There are no clear inflections in the  $D^{-1}(T)$  plots for sample FBM (Figure 6e).  $D_{010}$  is greater than  $D_{001}$  at all temperatures, implying that this sample has a  $C\bar{1}$  structure, and cooled quickly enough to preserve that  $C\bar{1}$  structure.

In sample FLL,  $D_{010}$  appears to exceed  $D_{001}$  at room temperature and above 1400 K (Figure 6f). However, the error bars for  $D_{001}$  and  $D_{010}$  in sample FLL overlap at room temperature and again at temperatures greater than 1100 K. Unlike the other samples,  $D_{\perp}$  is similar to the other orientations, being in between  $D_{001}$  and  $D_{010}$  at temperatures below 1000 and above 1400 K, but lower than  $D_{001}$  and  $D_{010}$  between those temperatures. The temperatures of the 1400 K crossover corresponds to the transition between the  $I\bar{1}$  and  $C\bar{1}$  structures, and the crossover is due mainly to a decrease in  $D_{001}$ . Data scatter and large error bars hide any clear inflections. However,  $D_{010}$  drops at  $\sim 1000$  K and  $D_{001}$  drops at  $\sim 1200$  K, the temperature of the  $e_1$  to  $C\bar{1}$  transition expected at 1200 K. The Lake County sample cooled relatively slowly within a thick basaltic lava flow. This explains the weak  $e$  reflections in the single-crystal x-ray photographs (Wenk 1980). A decrease of  $D_{001}$  as temperatures approach 1600 K results from premelting effects.

We expect to see the effects of the  $P\bar{1}$  to  $I\bar{1}$  transition in sample FMA. The  $D^{-1}(T)$  data show an inflection in (001) at about 525 K (Figure 6g), slightly higher than expected for the transition (Figure 1). No clear inflection occurs in the (010) data.

## Thermal diffusivity and thermal expansivity

The volume coefficient of thermal expansion ( $\alpha_v$ ) was calculated for different members of the plagioclase series from measured volumes from Hovis et al. (2010) and Tribaudino et al. (2010), using:

$$\alpha_v = \frac{1}{V_0} \frac{\partial V}{\partial T} \quad (2)$$

where  $V_0$  is the volume at room temperature. Linear fits to  $V(T)$  were appropriate and used to compute  $\alpha_v$ . To determine dependence of  $\alpha_v$  on An content, the two variables were plotted and linearly fit, using different fits for An<40 and An>40 (not shown).

Values of room temperature  $D^{-1}$  are compared with  $\alpha_v$  in Figure 7. As seen by the disagreements of values calculated from different volume data, large uncertainty exists in  $\alpha_v$  (Figure 7). Nonetheless, ~~a clear trend shows that~~ samples with lower thermal expansion coefficients have higher  $D^{-1}$  (lower  $D$ ) values. This is opposite of what was seen in halides (Yu and Hofmeister 2011) and endmember perovskites (Hofmeister 2010), where  $\alpha_v$  and  $D^{-1}$  are positively correlated. In those minerals, higher  $\alpha$  means the lattice is more responsive to temperature, hence causing more phonon scattering and higher  $D^{-1}$ . In plagioclase, disorder has reversed the trend. Samples with An>40 plot along different trends than do more sodic samples. Although offset, the trends do have similar slopes. The different trends reflect the different structures for minerals with these An contents; this break is <sup>roughly</sup> generally the boundary between  $C\bar{1}$  and  $I\bar{1}$ . Although lattices of more An-rich samples should be less responsive to  $T$ , effects of higher amounts of Al-Si disorder <sup>mask</sup> swamp the lattice impact on  $D$ . <sup>obscure?</sup>

<sup>collog.</sup>

Directional  $D^{-1}(T)$  should go as  $\alpha_L T$ , reflecting the fact that both are governed by anharmonic effects. Because thermal changes in length are small,  $\alpha_L$  is most accurate in the middle of the temperature range. Therefore, lengths of **a**, **b** and **c** for albite (Tribaudino et. al 2010) were plotted at temperatures  $>500$  K and linearly fit.

For the (010) and  $\perp$  samples,  $\alpha_L T$  and  $D^{-1}(T)$  increase similarly with temperature, as expected (Figure 8). This behavior was similarly seen in perovskites and halides (Hofmeister 2010; Yu and Hofmeister 2011). The slope of  $\alpha_L T$  for the **c** orientation is much less than that for  $D^{-1}(T)$ , which causes  $\alpha_L T$  along **a** $>$ **b** $>$ **c**, but  $D^{-1}$  along **a** $>$ **c** $>$ **b**. The mismatch in slopes for the (001) sample indicates that additional phonon scattering, probably due to disorder upon heating and not the expected lattice effect, enhances  $D^{-1}$  along this orientation. That disordering decreases  $D$  in albite mimics the fact that ordering (due to formation An-like domains, for example) increases  $D$  preferentially along **c**.

### Thermal conductivity

*pertains to*

Because thermal conductivity ~~is often used in~~ thermal and ~~other~~ geodynamic models, ~~we~~ *ing* can use our measured thermal diffusivities along with literature values of densities and heat capacities to calculate thermal conductivities ( $k$ ) using:

$$k = D \frac{c_p}{\rho} \quad (5)$$

Bulk thermal diffusivities of samples were calculated using:

$$D = \left[ \frac{1}{3} \left( \frac{1}{D_x} + \frac{1}{D_y} + \frac{1}{D_z} \right) \right]^{-1} \quad (6)$$

where  $D_x$ ,  $D_y$  and  $D_z$  are diffusivities along three orthogonal directions. Heat capacities vary only slightly for different members of the plagioclase solid solution (Figure 8). Nonetheless, thermal conductivities were calculated using An-specific heat capacity values from Benisek et al. (2009). Densities were calculated using temperature-dependent molecular volumes, which were assumed to vary linearly with An content, using albite and anorthite values from Holland and Powell (1998). Thermal conductivities are not very sensitive to the choice of density. Measured volumes from Tribaudino et al. (2010) give very similar  $k$  values. The resulting thermal conductivity values change little with temperature for all but the most albite-rich plagioclase (Figure 9).

Because  $D$  was only measured in two of the three orientations,  $k$  of FSU was not calculated. Thermal conductivity of the most Ca-rich sample (FMA) is also not shown in Figure 9 because only two orientations were measured. If those two orientations are used to calculate average  $D$ , then  $k$  ranges from 1.37-1.57  $\text{Wm}^{-1}\text{K}^{-1}$ . Including a third orientation that is 90% that of  $D_{010}$  results in a similar  $k$  value ranging from 1.33-1.50  $\text{Wm}^{-1}\text{K}^{-1}$  for FMA.

### Comparison with previous measurements of plagioclase and other major rock-forming minerals

Although ~~albite and potassium~~ <sup>alkali</sup> feldspar minerals have been previously analyzed, measurements of plagioclase heat transfer properties are rare in the literature. An exception is a study by Magnitskiy (1971) of a “labradorite” (density of 2.67  $\text{g/cm}^3$ ) and an “oligoclase” (density of 2.63  $\text{g/cm}^3$ ). Specific An contents were not reported. Thermal diffusivities were measured to 1200 K with plane-periodic wave method, which involves one thermocouple attached to the sample; the samples were not oriented crystals. Their data is in decent agreement

with our measurements; the “oligoclase” values are slightly higher than our FON sample to 800 K, and their “labradorite” values are on the low end of our FLL and FLN measurements at temperatures up to 1000 K (Figure 10).

Linivill (1987) measured thermal diffusivity of samples from Madagascar ( $Ab_{99}An_1$ ,  $\rho=2.622$ ), Nain ( $Ab_{48.7}An_{48}Or_{3.3}$ ,  $\rho=2.695$ ), Lake St. John ( $Ab_{33}An_{65.5}Or_2$ ), and Lake County ( $Ab_{31}An_{68}Or_1$ ,  $\rho=2.71$ ) at low temperatures using a divided bar technique and to about 500 K using the modified Ångstrom method. The long axes of the samples were 010 in albite,  $11\bar{2}$  in the Nain sample, and  $20\bar{3}$  in the Lake County sample. Orientations for the Lake St. John sample were not given. Data from attained with the modified Ångstrom method are shown in Figure 10. Compared with our FLL and FLN samples, Linivill’s Lake County and Lake St. John data are slightly lower than ours, and Nain data are higher than ours, probably due to various amounts of radiative gains and contact losses in her technique.

When compared with other common rock-forming minerals, plagioclase has one of the lowest thermal diffusivities, both at room temperature and higher temperatures (Figure 11). Of the major families of rock-forming minerals, quartz and olivine have the highest thermal diffusivities. In general, thermal diffusivity is linked to the number of active infrared (IR) modes in a mineral along the direction probed, which is determined by number of atoms and structure in a given unit cell (Hofmeister, in review). Quartz and olivine have few modes compared to orthopyroxene and garnets, and thus plot higher in Figure 11. Interestingly, the correlation is not with the number of optic modes, but only with IR modes, and the degeneracy of the IR modes is not relevant (e. g., garnet has 237 optic modes, considering degeneracies). It is the individual peaks that have an effect. The correlation with infrared modes, and the fact that infrared modes involve a change in dipole moment, unlike Raman or inactive modes, suggests that heat



propagation can be described as an electromagnetic wave traversing the sample. This radiative component must act with phonon scattering to explain heat transfer in solids. The large number of infrared modes means high levels of photon emission and absorption in plagioclase samples, impeding heat transfer.

well written

## Conclusions

As in all minerals,  $D$  decreases upon heating as more phonons lead to increased phonon scattering and the shift of the blackbody curve leading to more photon emission and absorption. Additional changes in  $D(T)$  occur because of structural changes upon heating. For example,  $D$  drops in all samples during the transition to  $C\bar{1}$  symmetry. Fast heating and cooling during LFA measurements do not allow for atomic diffusion. Because inflections in the  $D(T)$  curves occur at temperatures expected for phase transitions, we conclude even fast heating results in reversible structural changes to the lattice.

Disorder accompanying Al/Si substitution causes  $D$  of plagioclase to decrease with increasing anorthite content. The decrease seems mostly continuous across the solid solution, regardless of the crystallization temperature and/or cooling history of the sample, although more ordered samples have slightly higher  $D$  values than less-ordered samples. This suggests that ordering/disordering dictated by structure at a given composition is minimal compared with ordering/disordering dictated by An contents.

Our results can easily be converted to thermal conductivity ( $k$ ) values, and used in models to address geologic problems. When combined with heat capacity and density,  $D$  give similar room temperature  $k$  values (between about 1.5 and 1.9  $\text{Wm}^{-1}\text{K}^{-1}$ ) for all plagioclase samples containing intermediate values of Ca. Because plagioclase  $k$  changes little with

temperature, inclusion of temperature derivatives is not as imperative as with other minerals. Plagioclase's insulating nature ( $D$  is lower for plagioclase (at all temperatures) than for other major rock-forming minerals) suggests that plagioclase will dictate lower bounds of  $D$  and  $k$  in plagioclase-bearing rocks, especially mafic rocks in Earth's crust.

### **Acknowledgements**

We wish to thank Artur Benisek and an anonymous reviewer for their insightful reviews that helped strengthen this manuscript. We also appreciate Paul Carpenter at Washington University in St. Louis for performing microprobe analyses of our samples and Cathleen Brown, Museum Specialist at the Smithsonian for providing some samples. Thanks also to the National Science Foundation, whose grants #0711020 and #0911428 funded this research.

## References

- Angel, R. J., Carpenter, M. A. and Finger, L. W. (1990) Structural variation associated with compositional variation and order-disorder behavior in anorthite-rich feldspars. *American Mineralogist*, 75, 150-162.
- Benisek, A., Dachs, E. and Kroll, H. (2009) Excess heat capacity and entropy of mixing in high structural state plagioclase. *American Mineralogist*, 94, 1153-1161.
- Branlund, J. M. and Hofmeister, A. M. (2007) Thermal diffusivity of quartz to 1000 °C: Effect of impurities and the  $\alpha$ - $\beta$  phase transition. *Physics and Chemistry of Minerals*, 34, 581-595.
- Carpenter, M. A. (1994) Subsolidus phase relations of the plagioclase feldspar solid solution. In I. Parsons, Ed. *Feldspars and their reactions*. p. 221-270. NATO ASI Series C Vol. 421, Edinburgh.
- Carpenter, M. A. (1991) Mechanisms and kinetics of Al-Si ordering in anorthite: I. Incommensurate structure and domain coarsening. *American Mineralogist*, 76, 1110-1119.
- Carpenter, M. A. and McConnell, J. D. C. (1984) Experimental delineation of the  $I\bar{1} \leftrightarrow C\bar{1}$  transformation in intermediate plagioclase feldspars. *American Mineralogist*, 69, 112-121.
- Foit, F. F. and Peacor, D. R. (1973) The anorthite crystal structure at 410 and 830° C. *American Mineralogist*, 58, 665-675.
- Grove, T. L. (1977) A periodic antiphase structure model for the intermediate plagioclases ( $An_{33}$  to  $An_{75}$ ). *American Mineralogist*, 62, 932-941.
- Hofmeister, A. M. (2011) Thermal diffusivity of spectroscopically characterized orthopyroxenes as a function of temperature and chemical composition. Submitted to *European Journal of Mineralogy*.
- Hofmeister, A. M. (2010) Thermal diffusivity of oxide perovskite compounds at elevated

- temperature. *Journal of Applied Physics*, 107, 103532 (20 pgs).
- Hofmeister, A. M. (2007) Thermal diffusivity of aluminous spinels and magnetite at elevated temperature with implications for heat transport in Earth's transition zone. *American Mineralogist*, 92, 1899-1911.
- Hofmeister, A. M. (2006) Thermal diffusivity of garnets at high temperature. *Physics and Chemistry of Minerals*, 33, 45-62.
- Hofmeister, A. M., Whittington, A. G. and Pertermann, M. (2009) Transport properties of high albite crystals, near-endmember feldspar and pyroxene glasses, and their melts to high temperature. *Contributions to Mineralogy and Petrology*, 158, 381-400.
- Holland, T. J. and Powell, R. (1998) An internally consistent thermodynamic data set for phases of petrologic interest. *Journal of Metamorphic Petrology*, 16, 309-343.
- Hovis, G. L., Medford, A., Conlon, M., Tether, A. and Romanoski, A. (2010) Principles of thermal expansion in the feldspar system. *American Mineralogist*, 95, 1060-1068.
- Johannes, W., Koepke, J. and Behrens, H. (1994) Partial melting reactions of plagioclases and plagioclase-bearing systems. In I. Parsons, Ed. *Feldspars and their reactions*. p. 161-194. NATO ASI Series C Vol. 421, Edinburgh.
- Linville, M. (1987) Glass-like thermal conductivity behavior in feldspars. PhD thesis, Cornell University, Ithaca, NY.
- Magnitskiy, V. A., Petrunin, G. I. and Yurchak, R. P. (1971) Thermal diffusivity of selected microclines and plagioclases between 300 and 1200 degrees K. *Doklady: Earth Science Sections*, 199, 25-27.
- McConnell (2008) The origin and characteristics of the incommensurate structures in the plagioclase feldspars. *The Canadian Mineralogist*, 46, 1389-1400.

- Mehling, H., Hautzinger, G. and Nilsson, O. and Fricke, J. and Hofmann, R. and Hahn, O. (1998) Thermal diffusivity of semitransparent materials determined by the laser-flash method: applying a new analytical model. *International Journal of Thermophysics*, 19, 941-949.
- Parsons, I. (2010) Feldspars defined and described: a pair of posters published by the Mineralogical Society. Sources and supporting information. *Mineralogical Magazine*, 74, 529-551.
- Pertermann, M. and Hofmeister, A. M. (2006) Thermal diffusivity of olivine-group minerals at high temperature. *American Mineralogist*, 91, 1747-1761.
- Pertermann, M. and Hofmeister, A. M. (2008) Thermal diffusivity of clinopyroxenes at elevated temperatures. *European Journal of Mineralogy*, 20, 537-549.
- Pertermann, M., Whittington, A. G., Hofmeister, A. M., Spera, F. J. and Zayak, J. (2008) Transport properties of low-sanidine single-crystals, glasses and melts at high temperature. *Contributions to Mineralogy and Petrology*, 155, 689-702.
- Prewitt, C. T., Sueno, S. and Papike, J. J. (1976) The crystal structure of high albite and monalbite at high temperatures. *American Mineralogist*, 61, 1213-1225.
- Tribaudino, M., Angel, R. J., Cámara, F., Nestola, F., Pasqual, D. and Margiolaki, I. (2010) Thermal expansion of plagioclase feldspars. *Contributions to Mineralogy and Petrology*, 160, 899-908.
- Wenk, H-R., Joswig, W., Tagai, T., Korekawa, M. and Smith, Bradley K. (1980) The average structure of An 62-66 labradorite. *American Mineralogist*, 65, 81-95.
- Yu, X. and Hofmeister, A. M. (2011) Thermal diffusivity of alkali and silver halide crystals as a function of temperature. *Journal of Applied Physics*, 109, 033516-1.

## Figure captions

### Figure 1

Phase diagram for plagioclase showing major structures (modified from Parsons (2010) and McConnell (2008), with the low to high  $C\bar{I}$  transition from Carpenter (1994)). Pe, Bø, Hü are the peristerite, Bøggliid and Hüttenlocher intergrowths, respectively.

### Figure 2

Thermal diffusivities versus temperature for (a) samples FON (filled gray), FBM (open black), and albite (filled black, from Hofmeister et al. (2009)), and (b) samples FLN (filled gray), FSU (filled black), FLL (open black) and FMA (open gray). Measurements made on (010) are shown as squares, on (001) are shown as circles, and on perpendicular sections are shown as triangles. Error bars are included, but many are smaller than the symbol size. Larger error bars for albite (001) reflect uncertainty due to excessively large sample thickness.

### Figure 3

Thermal diffusivity versus An content. Black symbols show values measured at room temperature, and gray symbols show values measured at about 1100 K (1061-1131 K). Measurements made on (010), (001) and  $\perp$  are shown with squares, circles and triangles, respectively.

### Figure 4

Thermal diffusivity values measured as sample FLN cooled from 1600 K (filled symbols) were higher than measurements made during heating (open symbols) until about 800 K, although

those made upon cooling at lower temperatures, as well as room temperature  $D$  measured many days later (010=cross, 001=diamond), were lower than the original measurements due to cracks in the sample. Measurements made on (010), (001) and  $\perp$  are shown with squares, circles and triangles, respectively.

#### Figure 5

Phase diagram (from Figure 1) showing the direction of maximum  $D$  for the different structures. Location of the  $C\bar{1}/I\bar{1}$  boundary (heavy black line) agrees with data from Carpenter et al. (1984). Pe, Bø, Hü are the peristerite, Bøggliid and Hüttenlocher intergrowths, respectively.

#### Figure 6

Inverse thermal diffusivities for samples (a) albite, (b) FSU, (c) FON, (d) FLN, (e) FBM, (f) FLL and (g) FMA. Approximate positions of phase transitions (long vertical lines) and the solidus (if within the shown temperature range; double vertical line) are marked (from Figure 1). Measurements made on (010), (001) and  $\perp$  are shown with squares, circles and triangles, respectively. Fits from Table 2 are shown as lines. Arrows in figures 6c and 6f show the decrease in  $D$  due to melting or premelting. Larger error bars for albite (001) reflect uncertainty due to extreme sample thickness.

#### Figure 7

Correlation of room temperature values of  $1/D$  (averaged for the three orientations) with  $\alpha_v$ . Because only two orientations were measured, samples FLC and FMA are not shown in the diagram.  $\alpha_v$  was calculated using data from two different sources, squares= Tribaudino et. al

(2010) and circles = Hovis et al. (2010). Linear fits to samples with An<40 and An>40 are shown (grey=Tribaudino; black= Hovis).

#### Figure 8

$D^{-1}(T)$  using fits from Hofmeister et. al (2009) and  $\alpha_L T$  calculated from unit cell parameters (Tribaudino et al. 2010) for albite to high temperature.

#### Figure 9

Heat capacities (dashed lines) are compared with thermal conductivities (various solid and dotted lines) for plagioclase samples. Albite heat capacity is show in black, and thermal conductivity is shown with heavy black line. Also shown are thermal conductivities of FON (heavy dark gray), FBM (thin black), and FLL (long dash-dot), all calculated using data from Holland and Powell (1998). Most thermal conductivities calculated with volumes from Tribaudino et. al (2010) are similar, as shown for albite (dotted black). FON (gray dotted) shows more dissimilarity.

#### Figure 10

Comparison of our data (shaded=FON and outlined box=FLL and FLN) with data for “labradorite” (squares) and “oligoclase” (circles) samples from Magnitskiy (1971), and for samples from Nain (squares with crosses), Lake St. John (squares with diagonals) and Lake County (open squares) from Linvill (1987).

#### Figure 11



Summary of thermal diffusivity of important mineral families; plagioclase  $D$  values (triangles) are among the lowest of all rock forming minerals, both at room temperature ( $D_{298}$ ) and at high temperature ( $D_{highT}$ ). Plagioclase  $D_{highT}$  was measured at  $\sim 1350$  K for all samples in this study (does not include albite, FLC, FLT or FMA). Data for all orientations of other minerals are plotted along with lines of best fit; data were taken from the following references and used the following values for  $D_{highT}$ : quartz (open squares), with highT value from  $\beta$ -quartz at  $\sim 1100$  K (Branlund and Hofmeister 2007); olivine (gray diamonds), used “high temperature”  $D$  (Table 2 in Pertermann and Hofmeister 2006); clinopyroxene (black squares), used  $D_{sat}$  (Pertermann and Hofmeister 2008); orthopyroxene (square with X), used  $D$  at  $\sim 1200$  K (Hofmeister, 2011); garnet (gray dots), used  $D_{sat}$  (Hofmeister 2006); spinel (black dots), used  $D$  at  $\sim 1000$  K (Hofmeister 2007). Sanidine ( $D_{highT}$  at  $\sim 1200$  K) and albite ( $D_{highT}$  at  $\sim 1075$  K) mark the alkali feldspar (open circles) trend (from Pertermann et al. 2008 and Hofmeister et al. 2009, respectively). Only single crystals with high temperature measurements of multiple orientations were plotted. The lines of best fit for clinopyroxene and orthopyroxene overlap, and are labeled “pyroxene.” Trends correlate with number of infrared (IR) modes as labeled.